



Rock physics and geomechanical application in the interpretation of rock property trends for overpressure detection

Dorcas S. Eyinla^{1,2} · Michael A. Oladunjoye¹ · Abel I. Olayinka¹ · Boris B. Bate¹

Received: 29 June 2020 / Accepted: 5 November 2020 / Published online: 21 November 2020
© The Author(s) 2020

Abstract

One of the complexities of geomechanical study is in the classification of rock's properties and overpressured intervals—a knowledge which is not only essential for well safety and cost-effective drilling, but crucial in evaluating exploration risk factors and ensuring a successful hydraulic fracturing program. In this study, a more robust prediction of reservoir pressure regime is presented, where the geomechanical distributions of the rock give a distinct correlation. Three wells from the Niger Delta Basin were studied using empirical equations to estimate the elastic properties, wave velocities and the rock physics parameters for each well. From the results obtained, the velocities of compressional wave (V_p) and shear wave (V_s) decrease as porosity increases. Also, a linear correlation exists between Poisson's ratio and V_p/V_s , where both variables showed distinct behavior and similar trend serving as useful tools for lithology identification. Another significant observation is the acoustic impedance of the materials which decreases with increasing porosity. Meanwhile, the depth plot of the impedance showed divergence and scattering away from the supposed linear trend. While inhomogeneity of the rock materials and disequilibrium compaction of sediments may account for this scattering, the variation of geomechanical distributions in this study revealed that pore pressure has a first order effect on the elastic strength of formations, also, under normal pore pressure conditions, acoustic impedance increases linearly with depth.

Keywords Lithology identification · Rock physics · Acoustic impedance · Linear divergence · Overpressure

Abbreviations

ρ_b	Density (g/cm^3)
Δt_s	Shear interval transit time ($\mu\text{s}/\text{ft}$)
S	Shear modulus (psi)
P	Poisson's ratio
B	Bulk modulus (psi)
Y	Young's modulus (psi)
ϕ_D	Porosity estimated from Density log
ϕ_{AC}	Porosity estimated from Acoustic log
PP	Predicted pore pressure (psi/ft)
I_p	Compressional wave acoustic impedance $\text{g cm}^3 (\text{ft}/\text{s})$

Introduction

Drilling through overpressure formations poses numerous challenges and risks to operations if the properties of the material are not accurately predicted prior to drilling (Zhang 2019). Adequate knowledge of the geomechanical properties of hydrocarbon reservoirs play an important role in designing recovery well, enhance recovery, and in safe drilling (Abijah and Tse 2016; Saikia et al. 2018). From previous studies (e.g. Streit and Hillis 2004; Archer and Rasouli 2012; Eyinla and Oladunjoye 2014, 2018; Eshkalak et al. 2014; Vilarrasa et al. 2016; Abijah and Tse 2016; Kumar et al. 2017; Turner et al. 2017; Feng et al. 2018), these applications often include the predictions of overpressure and sand production, modeling of rock's fracability during hydraulic fracturing, and in the estimation of injection-induced seismicity during fluid injection. Thus, the ability to safely plan hydraulic fracturing program and drill through abnormal pressure intervals require a multiple approach to understand the dynamics of the overpressure mechanisms (Zhang 2019).

With hydraulic fracturing stimulation of unconventional reservoirs, production is optimized through the creation of

✉ Michael A. Oladunjoye
ma.oladunjoye@ui.edu.ng

¹ Petroleum Geosciences Unit, Department of Geology,
Pan African University Life and Earth Sciences Institute,
University of Ibadan, Ibadan, Oyo State, Nigeria

² Department of Earth Sciences, Adekunle Ajasin University,
Akungba-Akoko, Nigeria

a connected stimulated rock volume for higher conductivity (Maulianda et al. 2019). Hydraulic fracturing treatment stands out as one of the most efficient matrix stimulation techniques being adopted for enhanced oil recovery (Shafiq and Mahmud 2017; Kolawole and Ispas 2019). Formation fracturing pressure is one of the key parameters used in hydraulic fracturing design, and the magnitude of this parameter depends on formation depth and the material properties (Guo et al. 2007). Generally, the unconventional (tight) reservoirs differ greatly from conventional reservoirs as a result of their deeper depth of burial, strong diagenetic properties, huge heterogeneity, reduced porosity, abnormal pressure with low permeability, and poorly developed natural fractures (Xue et al. 2014; Wang et al. 2016; Feng et al. 2018). Therefore, the nature of fracture propagation and hydraulic fracture initiation in a naturally fractured reservoir is influenced by the properties of the natural fractures, pore pressure and in situ stresses. Failure to present an accurate measurement and estimations of these parameters for a reservoir subjected to hydraulic fracturing might result in well instability, poor initiation of hydraulic fracture, poor fracture propagation, well perforation failure, casing collapse, sanding, and suboptimal production level (Cook et al. 2007; Denney 2011; Taheri-Shakib et al. 2019). Also, formation damage is harmful to the recovery process as this could lead to massive pressure drop around the vicinity of the wellbore (Shafiq et al. 2019).

While it is possible to carry out laboratory measurement of these properties, the amount of sample size being considered using this method is small in most cases. Meanwhile, the isolated samples may not be sufficient to represent the elastic regime throughout the reservoir owing to the sample size (Saikia et al. 2018). Consequently, geomechanical studies are performed often on a well correlational basis, which could later be used as calibration points in converting 3D seismic data to create geomechanical models. Overpressure in hydrocarbon unit represents one of the major challenges facing production and enhanced recovery processes because of their impact on drilling safety, well placement, cost-effective drilling and field development strategies (Kukla et al. 2011). Geomechanical analysis and reservoir modeling are tools employed to study the difference between the fluid pressure measured in a stratigraphic unit and the 'normal' hydrostatic fluid pressure in the pore structure. A technique for predicting pore pressure and associated fracture gradient would be helpful in selecting adequate mud weight to ensure well and drilling safety, in preventing the use of excess mud weights leading to fracture or losses, in preventing hole collapses and to assist in correct designing of casing scheme to ensure optimum completion and maximum productivity (Basu et al. 1994; Law and Spencer 1998; Babu and Sircar 2011). The geomechanical knowledge and pressure level would also afford the opportunity to pre-determine any

sand production into a borehole, a problem which has been identified in drilling operations for long as it affects well productivity and the drilling equipment (Ispas et al. 2012; Zhou et al. 2016; Kolawole et al. 2018).

The origin of overpressures in the field of study has been attributed mostly to disequilibrium compaction of sediments (Swarbrick and Osborne 1998; Chukwu 2017; Nwozor et al. 2017; Ogunsakin et al. 2019). Thus, an appropriate design of a stable wellbore, especially when high-volume fluid injection is proposed, can only be achieved when the effects of the overpressure in the targeted zone have been thoroughly considered during the stages of well planning. The production from low permeable or unconventional reservoirs like tight sands, shale gas and carbonates, has become possible and more successful primarily because of various injection and hydraulic fracturing processes which have greatly improved the fault permeability, creating room for more recovery. As formation pressure in rocks changes due to the varying tectonic history and burial conditions, the resulting effect is often seen in the response of the reservoir to fluid injection and artificial fracturing (Feng et al. 2018; Eshkalak et al. 2014; Fan et al. 2016; Abijah and Tse 2016; Eyinla and Oladunjoye 2018). Nevertheless, the inherent strength of rocks has a direct correlation with the elastic properties, which has been observed to be a good source of information regarding the pressure state and sanding rate during production (Dresser Atlas 1982; Eyinla and Oladunjoye 2014).

Another important useful tool in studying rocks and their features is the acoustic impedance, which can be obtained from seismic data (Saputro and Haris 2017), and from wells using sonic and density logs (Dresser Atlas 1982). While shale strength is primarily controlled by the degree of compaction (Lal 1999; and Eyinla and Oladunjoye 2018), the rock saturation condition has a great effect on the compressional velocity (Maleki et al. 2014). Hence, as acoustic impedance relates the velocity of wave travel in rocks and the density of the material, the level of compaction of the sediments can indirectly correlated with the value of the acoustic impedance, and thus, the problem of overpressure and fluid saturation in sedimentary rocks can be similarly be addressed using this property. Additionally, reports have established that in most sedimentary environments, velocities and densities of siliciclastic rocks increase with depth, and this trend is often due to progressive mechanical compaction which in turn would yield porosities reduction (Avsath et al. 2003). With this knowledge, a more robust geomechanical study which can link the velocity of rocks with the degree of overcompaction of sediments and overpressure can be achieved.

Previous report from the same study area by Eyinla and Oladunjoye (2018) has considered the interrelationship between formation strength and fracture pressure, and the various patterns of the cross-plots proposed an interplay

of disequilibrium compaction. However, several drilling problems which are related to wellbore stability are also linked to improper study of the pore pressure regime. Thus, this study presents a further systematic approach for predicting overpressured zones in the formation by interpreting the correlation and specific trends of geomechanical properties and rock physics parameters estimated from each sampled interval based on empirical correlations using physical properties derived from wireline logs data. Trend analyses in this work involve depth variations of porosity, elastic properties, densities and acoustic impedances of the formation.

The study area is Akas Field which falls within Tertiary sediments of the Niger Delta Basin in Nigeria with three distinct Formations Akata Formation, Agbada Formation and the Benin Formation (Tuttle et al. 1999). The Akata Formation (base of the delta) is of marine origin composed of thick shale sequences (including turbidite sand, and minor amounts of clay and silt) serving as potential source rock. The Agbada Formation is the major petroleum-bearing unit, consisting of paralic siliciclastics, mainly shelf deposits of alternating sands, shales and mudstone over 3700 meters thick, which also represents the actual deltaic portion of the sequence. In the lower Agbada Formation, shale and sandstone beds were deposited in equal proportions, however, the upper portion is mostly sand with only minor shale interbeds. The Benin Formation is a continental latest Eocene to Recent deposit of alluvial and upper coastal plain sands that are up to 2000 m thick. The topmost layer is predominantly nonmarine upper delta plain sandstone. The various units of the Niger Delta are shown in Fig. 1. Considering the geological history of the study area where overpressure has frequent occurrence, virtually all the geologic events which contribute to the accumulation and preservation of overpressure are available in the basin (Owolabi et al. 1990; Stacher 1995; Udo et al. 2015). The rate of sediment instreaming to the basin is very high which makes the basin unstable, and obviously still subsiding till date. The resulting high sedimentation rate and burial history prevent adequate settlement and dewatering, which causes the formation to develop abnormally high porosity and high fluid content leading to a buildup of overpressured intervals when lithification begins (Stacher 1995). The Akata Formation consists of highly undercompacted and overpressured marine shales (Fig. 1) with fluids which is constantly subjected to high overburden stress. Based on the depositional sequence, even a little overburden stress exerted on the Akata shale would yield considerable quantity of fluid to the adjacent reservoir rocks. Also, having established that the prevailing trapping mechanism in the Niger Delta is the growth fault, the implication of this is that the post-depositional

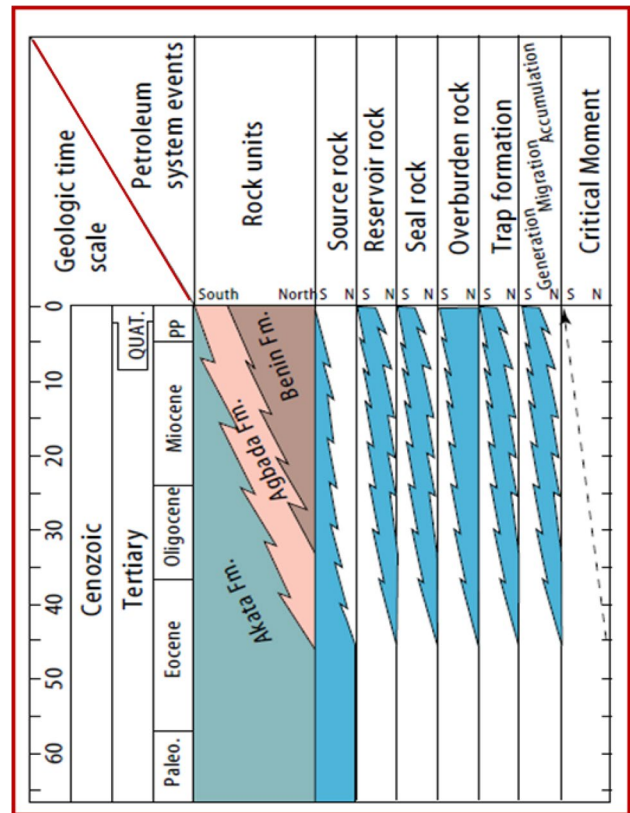


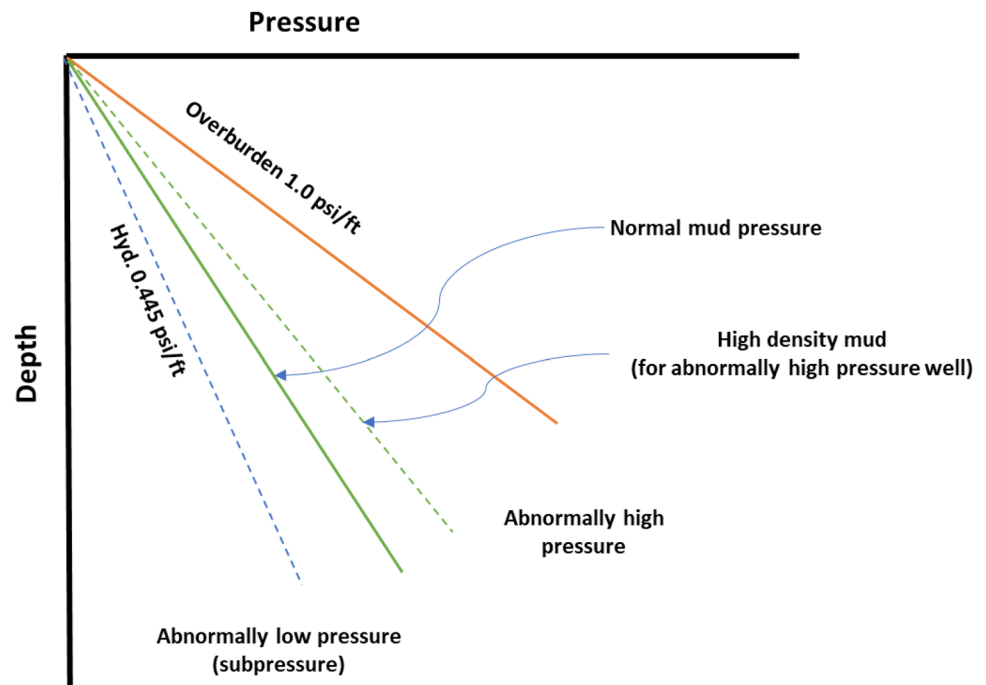
Fig. 1 Events chart for the Niger Delta (Akata/Agbada) Petroleum System (Modified after Tuttle et al.1999)

processes will build up excess reservoir pressure (Osinowo et al. 2015).

Basic theory and methodology

The various kinds of reservoir pressure usually encountered while drilling have been broadly divided into three main components: Hydrostatic pressure, Overburden pressure and Formation pressure as shown in Fig. 2. The reservoir fluid pressure found in the rock pores is regarded as the formation pressure while the overburden pressure is the combined pressure exerted by the rock formation (rock matrix) and the reservoir fluid (fluids in the pore space) overlying the formation. This pressure increases with depth and is also called the vertical stress (Chopra and Huffman 2006). Reservoir pressure controls the gas capacity and the overall reservoir behavior, and it consists of two main components: lithostatic pressure and hydrostatic pressure (Satter and Iqbal 2016). The lithostatic pressure is a consequence of overburden stress, while hydrostatic pressure is the component of the reservoir pressure resulting from the effect of pore fluid. Additional, lithostatic pressure is a function of rock density and is mostly ranges between 22.7 and 25 KPa/m (that is,

Fig. 2 Components of Pressure and their Relations (Modified from Ismail 2010)



1.0 and 1.1 psi/ft) in coal-bearing reservoir (McKee et al. 1984), whereas in normal hydrostatic gradient, the value in fresh water is 9.77 KPa/m (0.43 psi/ft), while the value in sea water is somewhat higher at 10.45 KPa/m (0.46 psi/ft). This research adopted hydrostatic gradient threshold value at 0.445 psi/ft, as shown in Fig. 2, being the reported average value for the study area. Pore pressure gradient is regarded as the ratio of the formation pressure to the depth and is often expressed in units of psi/ft or the equivalent of mud weight units in pounds per gallon (Chopra and Huffman 2006). Thus, pore pressures which are found to lie above or below the normal level of pore pressure gradient line are called abnormal pore pressures. From past works (Nwozor et al. 2013; Ichenwo and Olatunji 2018; Emudianughe and Ogagarue 2018), these formation pressures may be either subnormal (i.e. less than 0.445 psi/ft) or overpressured (i.e. greater than 0.445 psi/ft). The mechanisms which generate these abnormal pore pressures in subsurface reservoirs can be somewhat complex depending on the tectonic history, fluid expansion mechanism, and material constituents (Kukla et al. 2011; Satti et al. 2015).

Well logs obtained from well drilling are the most applicable and extensively used in the construction of rock models in rock strength study, and in delineating geopressures (Dutta 2002; Abijah and Tse 2016). Adopting wireline logs for estimating elastic and inelastic properties of rocks produce satisfactory results because the logs present a representation of the entire vertical section of the reservoir rocks, hence, they give a direct measurement of the petrophysical properties, and an ideal method of obtaining geomechanical data (Azizi and Memarian 2015; Abijah and Tse 2016). The

works of Liu et al. (2012) and Eyinla and Oladunjoye (2014, 2018) reported that sonic (acoustic) log contain information which can be helpful in determining the mechanical properties of rock. The velocity of compressional wave depends on the elastic properties of the matrix rock and fluid (Garia et al. 2019), therefore the measured slowness also varies, depending on the composition and microstructure of the matrix, the type and distribution of the pore fluid and the porosity of the rock (Dresser Atlas 1982).

Before geomechanical parameters are predicted, certain petrophysical properties are generated from the well logs. These parameters include: Porosity (from Density log and Sonic log), volume of shale, interval transit time of compressional sonic, and overburden gradient. The elastic properties of rocks and its relationship with velocity of wave provided a relationship through which geomechanical parameters are estimated using already established equations. A comprehensive study by Eyinla and Oladunjoye (2018) have presented clear procedures for estimating these rock properties from well logs, when sonic, density and gamma ray logs are available. Thus, this study adopted same procedure and approach for the estimation of the geomechanical parameters. The values represent change in the properties vertically along each wellbore, with no emphasis on lateral inhomogeneity. The three suites of well data used for the study contain wireline logs of density, sonic, gamma ray and resistivity data. Porosity values were estimated from porosity logs (density and sonic log) while the density values of each material were obtained from density log. Gamma ray log served for lithologic control which helped to distinguish the two major lithologic units (sands and shales).

Compressional and Shear wave velocities and geomechanical properties (Bulk modulus, Shear modulus, Young's modulus, and Poisson's ratio) were thus estimated using Eynla and Oladunjoye (2018) method.

Additionally, this study introduced certain rock physics analysis, which involves the study of the relationships between elastic parameters and petrophysical properties of the subsurface formation. Therefore, for this study, the parameters considered are: Density, P-wave impedance, P-wave velocity, S-wave velocity, Bulk modulus, Shear modulus, among others. The products of density and velocity (ρ and V) known as impedances (Telford et al. 1990) was calculated for the compressional wave as shown in Eq. 1.

$$I_p = \rho \times V_p \quad (1)$$

Shales can be distinguished from other lithology by using V_p/V_s ratio and the impedance of the compressional wave (I_p). Hence, reservoir with shale formation can be separated from non-reservoir shale by using these parameters (Kumar and Hoversten 2012). Consequently, cross-plots were designed using the estimated parameters to enable proper understanding of the different rock materials in the reservoir, the governing rock physics laws in place. Thus, these trends afford proper geological inference which have implications on overpressure prediction.

Results and discussion

The resulting geomechanical computations and pressured intervals are presented in Tables 1, 2 and 3 for the three wells while correlations of specific parameters from the evaluated results are made. From the results, it was observed that mechanical strength of the material varies with depth, and the order of this variation depends on the material constituents at each sampled interval. Also, a consistent trend in rock properties plots is observed, however, deviation from any expected trend is believed to be a resulting effect of abnormal pressure in the field.

Figure 3 shows that the shear wave velocity is linearly related to the compressional velocity across the three wells. That is, with an increasing value of shear wave velocity, the corresponding compressional wave velocity increases. This relationship gives a clearer understanding of how the elastic properties of rocks relate in terms of the seismic responses and material porosity. It suggests that as the porosity of the material increases, shear and compressional velocities decrease in an almost linear fashion (Castagna and Batzle 1985). In addition, the relationship of wave velocity of the material and porosity of the sediments has been established through the plot in Fig. 4. The trend plot showed that compressional wave velocities decrease with increasing porosity,

which implies an inverse relationship. Dolberg et al. (2000) reported that velocities are mostly sensitive to changes in porosity than change in fluid type or pressure in the reservoir. Thus, several reports have identified this relationship between wave velocities and the petrophysical properties of sedimentary rocks (e.g Assefa et al. 2003; Kahraman and Yeken 2008; Zhang et al. 2009; Al-Dousari et al. 2016 and Garia et al. 2019).

This study also revealed that both compressional velocity and shear velocity are dependent on porosity, since V_p and V_s have a similar decrease as porosity increases. From the trend plot of these two parameters, an imperfectly linear correlation is established, especially in Well 3. This is probably due to the variations in the values of elastic properties and pressure regime. A general rule is that with lower velocity (implying higher transit time), there is a corresponding rise in pore pressure (Zhang 2019). Figure 5 shows the plot of compressional velocity against density for the three wells, where velocity values increase with increasing density. The relationships between density and velocity provide an essential tool for geological analyses involving rock property parameters (Nwozor et al. 2017). The linear trends observed in this result indicate that the density and velocity of sands and shales increase with depth in normally pressured formations. However, the points which deviate from the supposed linear trend at certain intervals on the plot connote abnormal pressure zones. These points also correspond to the intervals which are observed to deviate from the linear trend in Fig. 4. In Well 1, these intervals with anomalous trend correspond to depth 7179 ft, 7549 ft, 7900 ft, 8900 ft, 9000 ft and 9250 ft. In Well 2, the intervals deviating from the linear trend are depth 6395 ft, 7195 ft, 7400 ft, 7600 ft and 8800 ft. In Well 3, these intervals are found at depth 6625 ft, 8025 ft and 8400 ft.

The plot of Shear modulus against Bulk modulus revealed that a linear correlation exists between the two elastic variables. Thus, in the three wells, materials which possess increased frictional resistance against shear stress also yield high resistance to compressibility (Fig. 6). Similarly, in Figs. 7 and 8, Bulk modulus and Shear modulus increase with decreasing porosity. This trend implies that the intervals with lesser porosities appear to be stiffer than highly porous layers, which agrees with the earlier reports by Gidley et al. (1989) and Tenthorey et al. (2003). Seemingly, the strength of any subsurface earth material is inversely correlated to porosity, which means that the ability of formation to support shear deformation and resist compression decrease with increasing porosity. The mechanical properties play a significant role in hydraulic fracturing of tight reservoirs, in terms of initiation and propagation of the hydraulic fracture (Josh et al. 2012; Li et al. 2015). Zones with high moduli strength and lower porosities would yield narrow fractures during hydraulic

Table 1 Estimated results for Well 1

Depth (ft)	ϕ_{AC}	ϕ_D	ρ_b (g/cm ³)	Δt_s (μ s/ft)	V_s (ft/sec)	V_p (ft/sec)	V_p/V_s	P	Y (psi) $\times 10^6$	S (psi) $\times 10^6$	B (psi) $\times 10^6$	I_p	PP (psi/ft)
6200	0.36	0.258	2.23	213	4686	8850	1.89	0.305	1.71	0.65	1.47	19736	0.404
6527	0.33	0.261	2.2	223	4475	8333	1.86	0.297	1.53	0.59	1.26	18333	0.515
6579	0.35	0.24	2.21	225	4449	8475	1.9	0.31	1.54	0.59	1.35	18730	0.503
7036	0.39	0.258	2.19	240	4175	8000	1.92	0.313	1.34	0.51	1.2	17520	0.604
7179	0.26	0.188	2.34	175	5703	10753	1.89	0.304	2.66	1.02	2.27	25162	0.113
7324	0.29	0.217	2.28	200	4994	9349	1.87	0.3	1.98	0.76	1.65	21308	0.433
7549	0.41	0.264	2.19	232	4307	8265	1.92	0.314	1.43	0.54	1.28	18100	0.63
7700	0.23	0.185	2.29	182	5506	10204	1.85	0.295	2.39	0.92	1.94	23367	0.341
7900	0.25	0.205	2.27	203	4928	9091	1.84	0.292	1.91	0.74	1.53	20637	0.548
8900	0.26	0.194	2.33	165	6066	11364	1.87	0.301	2.99	1.15	2.5	25342	0.262
9000	0.314	0.218	2.29	201	4968	9434	1.9	0.308	1.98	0.76	1.72	21604	0.603
9250	0.28	0.218	2.26	211	4747	8850	1.86	0.298	1.77	0.68	1.46	20001	0.703
9350	0.18	0.146	2.36	146	6867	12658	1.84	0.292	3.85	1.49	3.08	29873	0.158
10400	0.23	0.195	2.27	195	5137	9434	1.84	0.289	2.07	0.8	1.64	21415	0.716
10700	0.12	0.112	2.41	149	6732	12195	1.81	0.281	3.75	1.47	2.85	29390	0.429
11150	0.098	0.096	2.44	139	7177	12821	1.79	0.272	4.28	1.68	3.13	31283	0.406
11400	0.18	0.13	2.42	154	6491	12195	1.88	0.302	3.56	1.37	3.01	29512	0.526
11800	0.16	0.145	2.34	169	5924	10753	1.82	0.282	2.56	1.1	2.16	25162	0.699

Table 2 Estimated results for Well 2

Depth (ft)	ϕ_{AC}	ϕ_D	ρ_b (g/cm ³)	Δt_s (μ sec/ft)	V_s (ft/sec)	V_p (ft/sec)	V_p/V_s	P	Y (psi) $\times 10^6$	S (psi) $\times 10^6$	B (psi) $\times 10^6$	I_p	PP (psi/ft)
6000	0.327	0.247	2.23	210	4768	8929	1.873	0.3	1.77	0.68	1.48	19912	0.372
6395	0.319	0.218	2.32	183	5471	10417	1.904	0.309	2.44	0.93	2.13	24167	0.125
6595	0.385	0.268	2.2	226	4426	8403	1.899	0.308	1.51	0.58	1.31	18487	0.588
7000	0.324	0.232	2.26	202	4947	9346	1.889	0.305	1.93	0.74	1.66	21122	0.464
7195	0.233	0.192	2.34	162	6161	11364	1.845	0.292	3.07	1.19	2.46	26592	0.091
7400	0.335	0.249	2.24	214	4671	8772	1.878	0.302	1.71	0.65	1.44	19649	0.605
7600	0.223	0.169	2.41	155	6437	12048	1.872	0.3	3.48	1.34	2.9	29036	0.093
8566	0.299	0.229	2.26	196	5098	9524	1.868	0.299	2.05	0.79	1.7	21524	0.653
8800	0.091	0.097	2.47	132	7585	13333	1.758	0.261	4.8	1.9	3.35	32933	0.11
8950	0.179	0.158	2.4	153	6529	11905	1.823	0.285	3.52	1.37	2.73	28572	0.409
9420	0.231	0.198	2.32	178	5627	10309	1.832	0.288	2.54	0.98	1.99	23917	0.667
9800	0.156	0.164	2.36	159	6293	11111	1.766	0.264	3.17	1.25	2.23	26222	0.641
10000	0.28	0.219	2.28	194	5163	9615	1.862	0.297	2.11	0.81	1.74	21922	0.785
10200	0.251	0.205	2.3	185	5410	10000	1.848	0.293	2.33	0.9	1.88	23000	0.768
10800	0.281	0.227	2.26	194	5144	9524	1.851	0.294	2.07	0.8	1.68	21524	0.837
11180	0.241	0.206	2.3	181	5512	10101	1.833	0.288	2.41	0.94	1.9	23232	0.821

Table 3 Estimated results for Well 3

DEPTH (ft)	ϕ_{AC}	ϕ_{D}	ρ_b (g/cm ³)	Δt_s (μ sec/ft)	V_s (ft/sec)	V_p (ft/sec)	V_p/V_s	P	Y (psi) $\times 10^6$	S (psi) $\times 10^6$	B (psi) $\times 10^6$	I_p	PP (psi/ft)
5800	0.432	0.268	2.21	230	4347	8403	1.933	0.317	1.47	0.56	1.35	18571	0.435
6000	0.482	0.337	2.13	239	4183	7937	1.897	0.308	1.31	0.50	1.13	16906	0.536
6400	0.432	0.278	2.20	229	4372	8403	1.922	0.314	1.45	0.55	1.30	18487	0.49
6625	0.428	0.347	2.16	239	4191	7752	1.850	0.294	1.32	0.51	1.06	16744	0.61
7050	0.423	0.308	2.15	222	4499	8475	1.884	0.304	1.52	0.58	1.29	18221	0.529
7355	0.364	0.297	2.19	200	5010	9259	1.848	0.293	1.90	0.74	1.53	20277	0.418
7600	0.368	0.305	2.16	208	4801	8850	1.843	0.291	1.72	0.67	1.38	19116	0.519
8025	0.405	0.356	2.03	226	4421	8065	1.824	0.285	1.37	0.53	1.06	16372	0.646
8200	0.336	0.297	2.15	190	5275	9615	1.823	0.285	2.06	0.80	1.59	20672	0.433
8400	0.337	0.234	2.34	220	4540	8621	1.900	0.308	1.69	0.65	1.47	20173	0.603
8620	0.277	0.258	2.23	171	5832	10526	1.805	0.279	2.60	1.02	1.96	23473	0.298
9036	0.378	0.356	2.00	225	4441	8000	1.801	0.277	1.35	0.53	1.01	16000	0.718
9300	0.332	0.318	2.15	172	5802	10417	1.795	0.275	2.47	0.97	1.83	22397	0.396
9600	0.233	0.183	2.32	199	5024	9346	1.860	0.297	2.04	0.78	1.67	21683	0.577
9800	0.282	0.264	2.22	177	5657	10204	1.804	0.278	2.43	0.95	1.83	22653	0.482
10200	0.359	0.348	2.10	161	6202	11111	1.792	0.274	2.76	1.08	2.03	23333	0.372
10500	0.187	0.14	2.38	180	5550	10417	1.877	0.302	2.56	0.98	2.15	24792	0.515
10800	0.241	0.238	2.25	157	6366	11364	1.785	0.271	3.11	1.22	2.26	25569	0.411
11200	0.196	0.222	2.26	144	6927	12048	1.739	0.253	3.64	1.45	2.46	27228	0.321
11500	0.138	0.155	2.33	164	6109	10638	1.741	0.254	2.92	1.17	1.98	24787	0.548

Fig. 3 P-wave velocity (V_p) vs S-wave velocity (V_s) for Well 1, Well 2 and Well 3

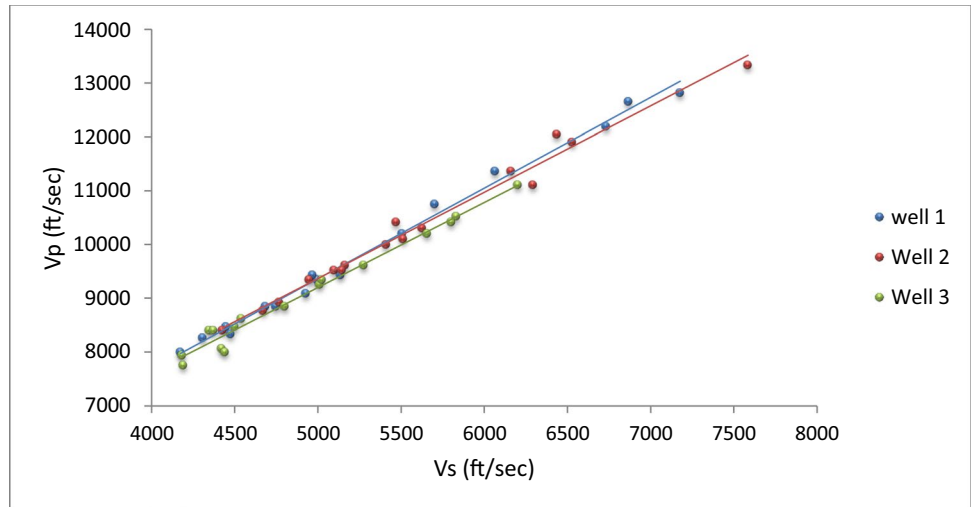


Fig. 4 Compressional velocity (V_p) vs porosity showing an inverse relationship

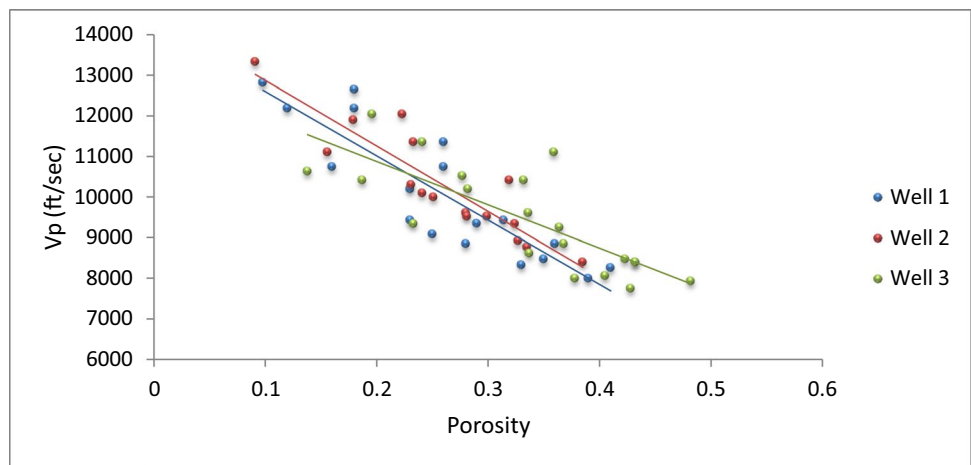
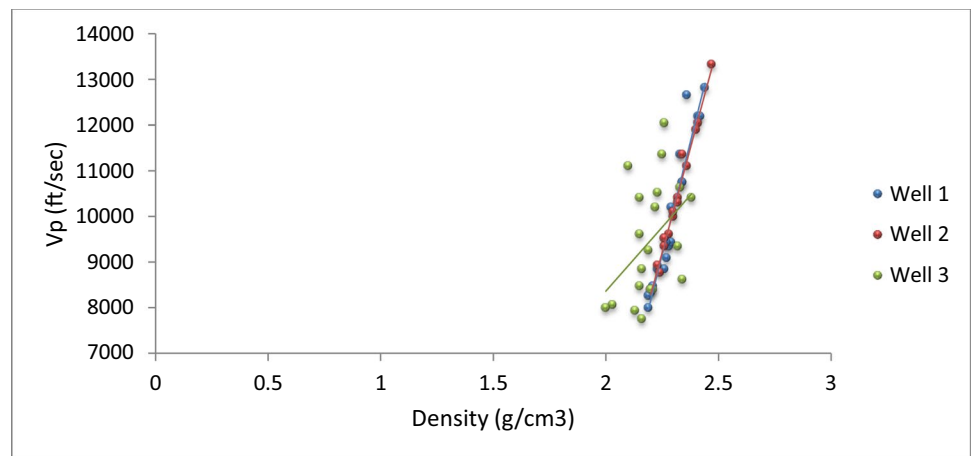


Fig. 5 Compressional velocity (V_p) vs density for the three wells



fracturing, whereas intervals with low moduli and high porosities would yield wider fractures. Report have suggested that hydraulic fractures are best when they are longer and narrower (Donaldson et al. 2013). Therefore,

in this case, the intervals with higher moduli are best targeted, as this would yield the narrow fractures for best performance. Another implication of the lower values of elastic strength is in the magnitude of seismicity during

Fig. 6 Plot of shear moduli and bulk modulus showing a linear relationship

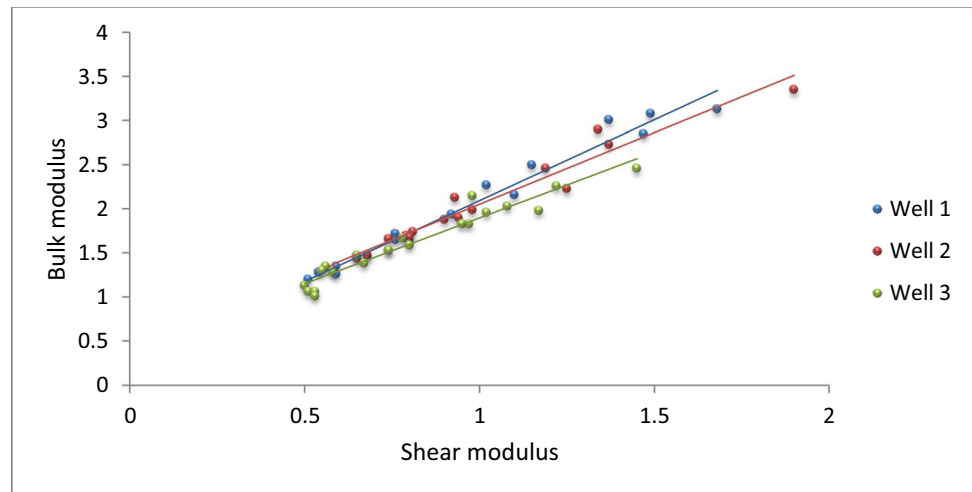


Fig. 7 Plot of shear modulus and porosity indicating a linear relationship

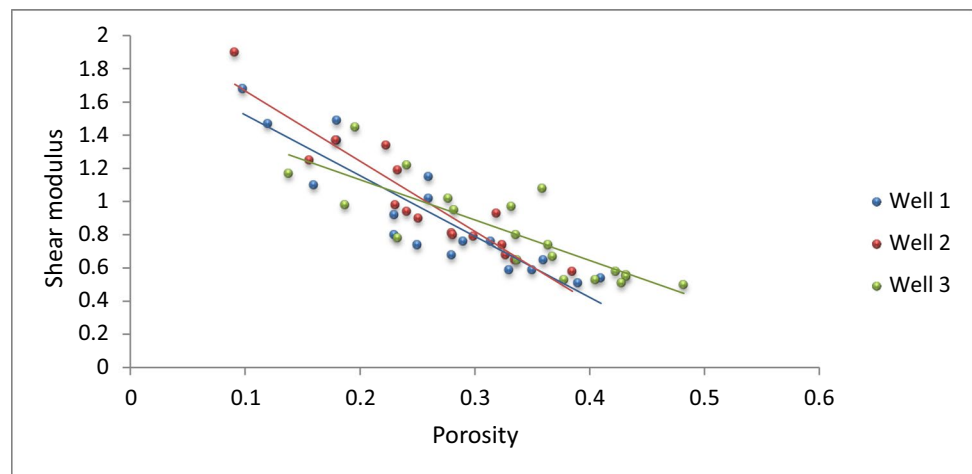
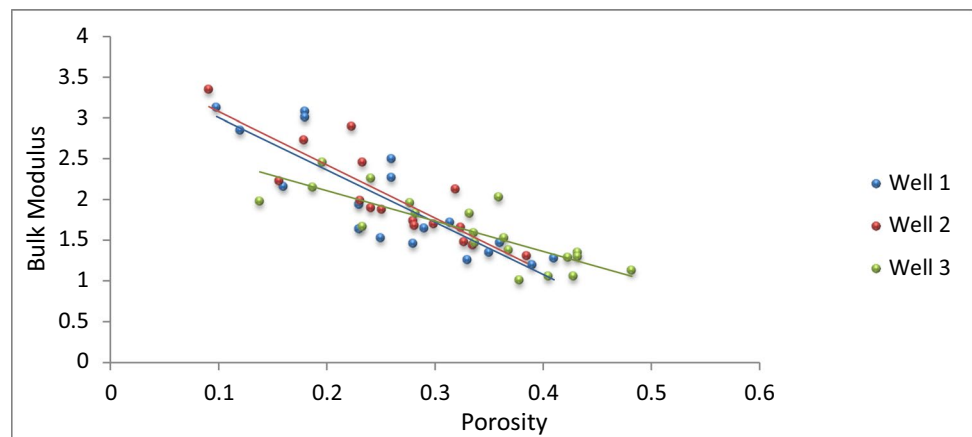


Fig. 8 Plot of Bulk modulus and porosity showing inverse relationship



injection (Gudmundsson 2004). Moreover, since the elastic properties of rocks are a significant parameter that best describe the mechanism that promote mechanical behavior of fault under rupture processes, the deformation of faulted block in terms of slip tendency and induced seismicity

is therefore a fundamental evidence of the elastic state of the rock. The intervals where lower elastic moduli are recorded would be highly unstable. Such soft matrix requires placement of multiple layers of proppant around the wellbore area. Whereas intervals with hard matrix,

where there is no embedment of the proppant, the fracture opening can be enhanced by using a monolayer of proppant (Donaldson et al. 2013). So far, the subsurface conditions that affect fractures orientations, failure modes and brittle behavior include the tectonic stresses and variability of elastic properties of the rock (Li et al. 2013). Thus, materials with low elastic properties would have higher magnitude of mechanical failure than formations with high elastic moduli.

The plots of Bulk and Shear moduli against density (Figs. 9, 10) both showed a direct relationship, indicating that dense materials are more rigid and incompressible than those which are less dense. Clearly, a slight increase in density increases the Shear and Bulk moduli largely, which shows how the elastic strength of the materials is highly sensitive to the material density. The changing behavior of these materials would play a major role in their response to injection and fracturing. Notably, previous study from the same wells by Eyinla and Oladunjoye (2018) showed that pore pressure and fracture gradient decrease as the three elastic moduli (Bulk, Young and Shear) increases. The intervals where the lower elastic properties have been observed are

also the same as the overpressured zones in this study. Thus, the pressured zones have been successfully linked with intervals where geomechanical strength is lowered.

Additionally, this study explored the gamma ray log to distinguish the geologic beds into sand and shale, however, the lithology was further characterized into geological beds using the ratio of compressional velocity to shear velocity (V_p/V_s). For this study, the velocity ratio was employed to make distinctions between the formation lithology and the result was compared with gamma ray lithology log. There was a good correlation between the two results, which established the validity of the calculated velocity ratio. Meanwhile, from the velocity ratio values in Tables 1, 2 and 3, and as shown in Fig. 11, the depth plot of V_p/V_s and Poisson's ratio revealed a perfectly linear correlation. This implies that both parameters have a relationship which can be adopted for lithology identification to discriminate the already established lithology of the formation (Wang et al. 2009). The values of V_p/V_s are consistently lower in sands than shales, and these shaly formations are already classified as overpressured sediments because of their properties and trends in other rock physics parameters. From Pickett (1963)

Fig. 9 Shear modulus against density showing direct relationship

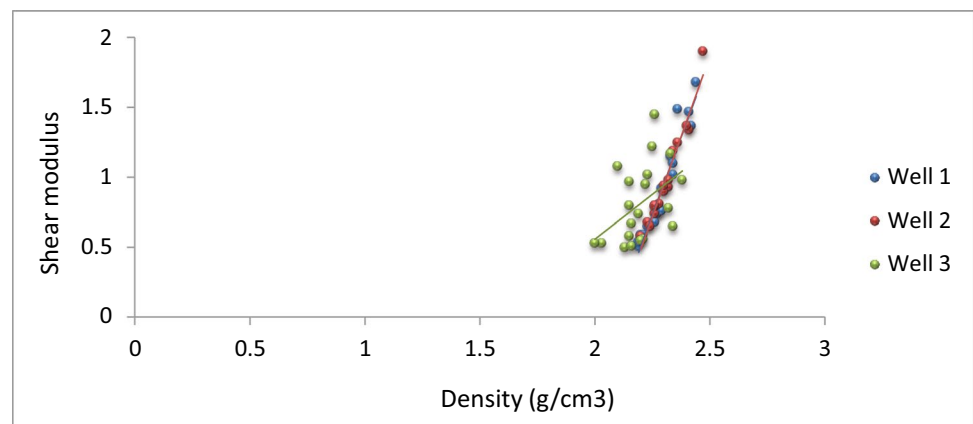


Fig. 10 Plot of Bulk modulus and density showing direct relationship

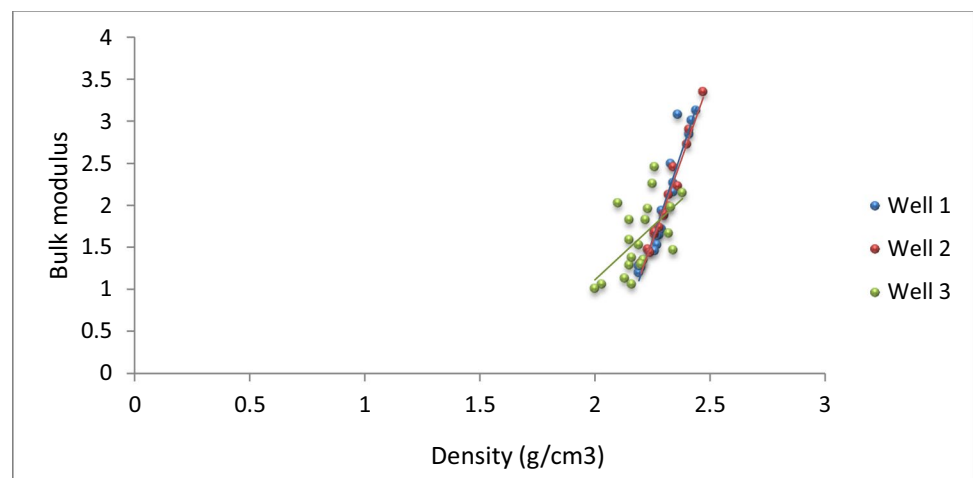
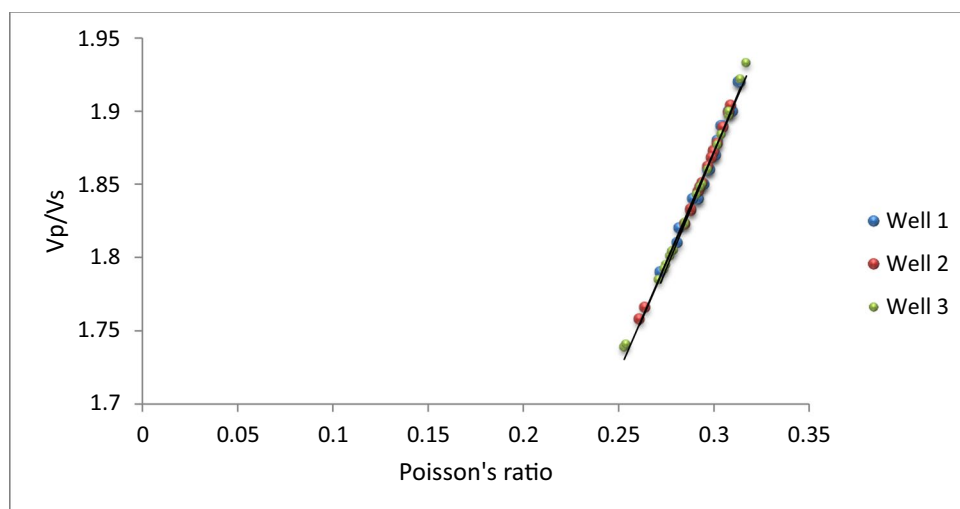


Fig. 11 V_p/V_s against Poisson's ratio showing linear relationship



reports, values of V_p/V_s ratios for different rock types vary (about 1.9 for limestone, 1.8 for dolomite, and 1.6–1.75 sandstones), and this velocity ratio is independent of the density of the rock. Therefore, this parameter be adopted with Poisson's ratio to compliment lithology identification. The correlations between the V_p/V_s and the corresponding Poisson's ratio values can also be applied in modeling and interpreting seismic data in terms of the particle's chemistry and lithology (Wang et al. 2009).

Also, Crain (2013) stated that low values of Poisson's ratio, about 0.10–0.30, are indicative of most sandstones and carbonates, hence, any rock materials which fall within these values are assumed to fracture relatively easily. However, those with higher values, ranging from about 0.35 to 0.45, are classified as shales, very shaly sandstone, and coal. Notably, a combined depth plot of V_p/V_s and P show increasing and decreasing sequence depending on the material encountered down depth (Figs. 12, 13 and 14). Generally, result shows that the intervals with high values of V_p/V_s and P indicate shale or shaly sands, and they are the

points indicated by black arrows on the plot. Meanwhile, these intervals also correspond to the highly pressured zones reported in other plots. Thus, an increase in V_p/V_s corresponds to increase in P , also, increase in shale content lowers V_p and V_s but increases V_p/V_s according to the report by Miller and Stewart (1990). It is believed that the materials present in the overpressured zone would be harder to fracture, thus, if hydraulic fracture is initiated without considering the material properties, these intervals would result in producing wider fractures during hydraulic fracturing. Nevertheless, the other intervals where V_p/V_s and P are not abnormally enhanced are classified as sandy or less shaly formations. Consequently, their material constituents are expected to yield narrow fractures with less fracture pressure during hydraulic fracturing (Eyinla and Oladunjoye 2014; Chen et al. 2016; and Eyinla and Oladunjoye 2018). The intervals with overpressure could also cause problem during hydraulic fracturing such as well bore instability, blowouts during drilling, diversion of hydraulic fracture path, poor fracture propagation and lost circulation are related to these

Fig. 12 V_p/V_s and Poisson's ratio against depth for Well 1 (Black arrows point at zones with high V_p/V_s values corresponding to shaly intervals and over pressure zones)

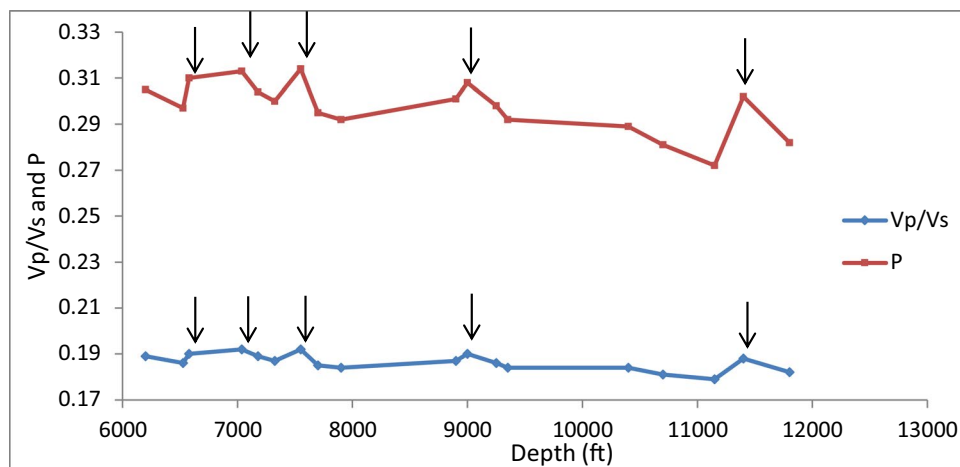


Fig. 13 V_p/V_s and Poisson's ratio against depth for Well 2 (Black arrows point at zones with high V_p/V_s values corresponding to shaly intervals and over pressure zones)

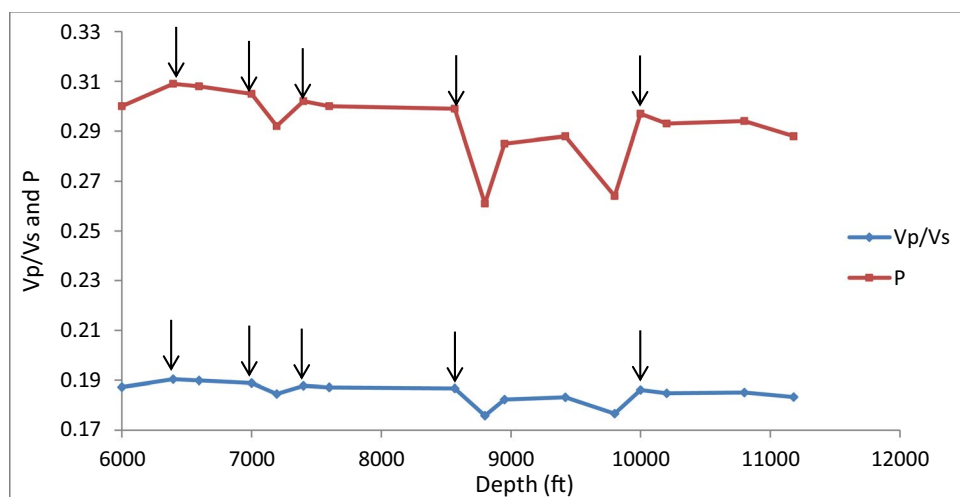
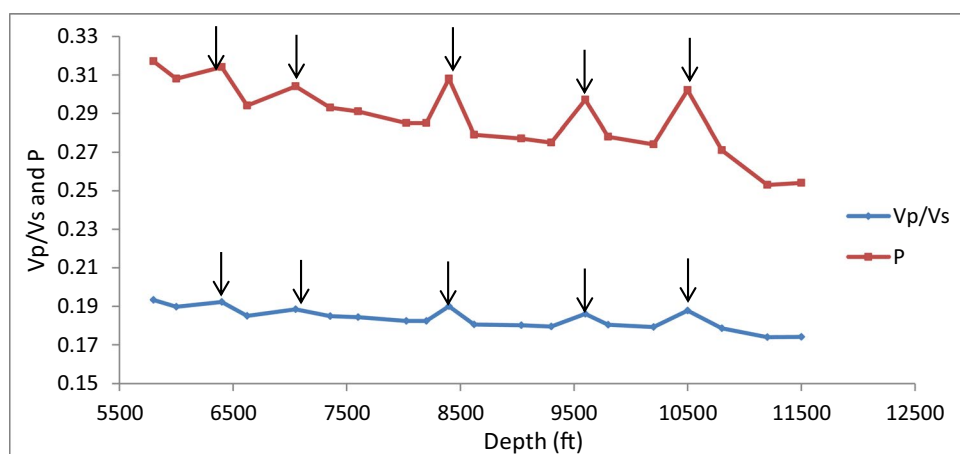


Fig. 14 V_p/V_s and Poisson's ratio against depth for Well 3 (Black arrows point at zones with high V_p/V_s values corresponding to shaly intervals and over pressure zones)



geostatic/hydrostatic pressure gradients issues in oil field rocks, and may be addressed and controlled by the adequate monitoring/adjustment of drilling fluid density during drilling operations.

Nevertheless, previous reports have indicated the possibility of identifying fluid or gas saturated reservoir using the V_p/V_s ratio. That is, a lower V_p/V_s may not only reveal an overpressured or shaly formation but may also be an indicative of a gas-bearing formation. This is because the presence of gas would increase the compressional transit time or slow down the compressional velocity of the material (Zhang 2019). The shear and compressional waves often give different response during passage through reservoir containing fluids and pressures, which implies that lower V_p/V_s can symbolize the presence of overpressure or gas saturation (Uyanik 2010). Thus, since compressional wave propagates in almost all kinds of medium (dry or saturated) whereas shear wave does not propagate in fluids, the porous medium saturated with fluids is expected to have a higher value of V_p above V_s , as rightly revealed in the result (Tables 1, 2 and

3). Consequently, the V_p/V_s ratio in a gas saturated environment is much lower than in liquid saturated reservoir (Tatham 1982). To clearly identify whether the interval with lower V_p/V_s in this formation is caused by overpressures or by gas effect, the shear transit time is examined, as described by Chilingar et al. (2002). The result in this study showed that gas in the reservoir has very little effect on the shear transit time, meanwhile, the effect of an overpressured formation causes both compressional and shear transit time to increase simultaneously (Fig. 3). Also, using the established behavior presented by Zhang (2019), overpressure in the formation is further identified where a very high shear wave velocity and shear transit time corresponds to a high pore pressure as shown in Figs 15, 16 and 17.

In addition, P-wave impedance, which is directly related to material incompressibility (Bulk modulus), decreases with increasing porosity (ϕ), as shown in Fig. 18.

This agrees with the study of Dolberg et al. (2000) and Chen et al. (2019), as their studies reported that acoustic impedance, acoustic resistance and acoustic reactance

Fig. 15 Plot of pore pressure and interval transit time against depth for Well 1 showing concurrent increase of both parameters

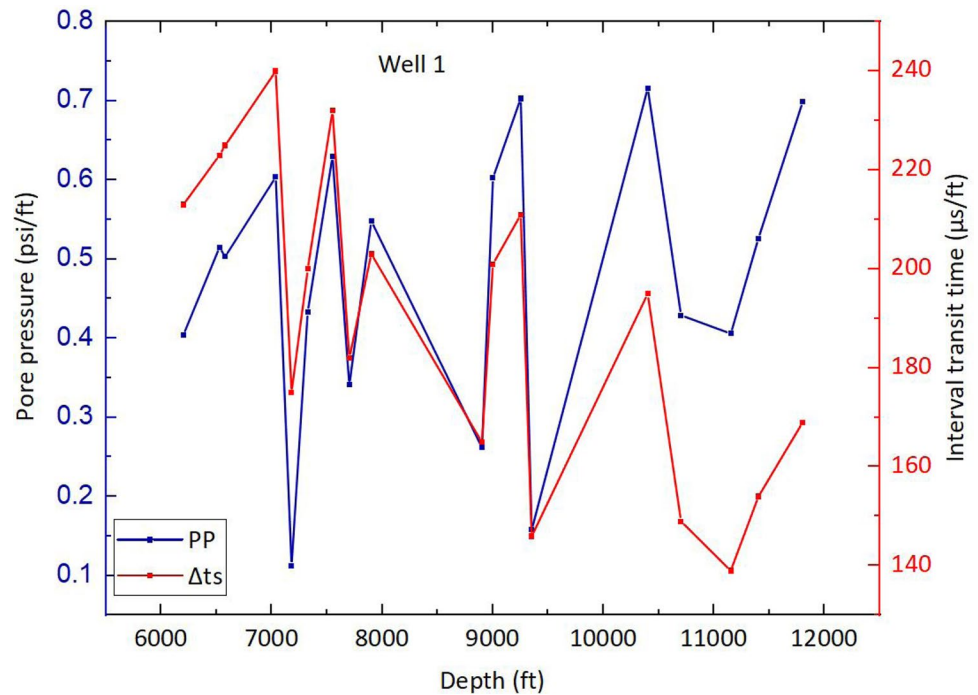
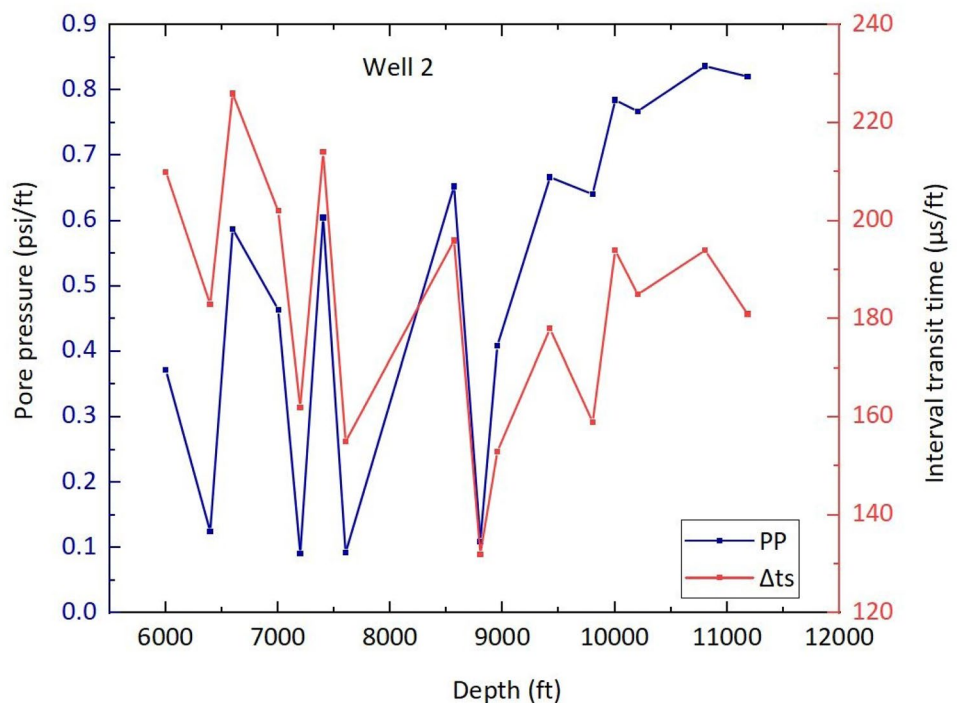


Fig. 16 Plot of pore pressure and interval transit time against depth for Well 2 showing concurrent increase of both parameters



decrease as porosity increases. They also reported that the differences in acoustic impedance in a well formation correlate with the variations in the porosity in an inverse relationship. The result obtained from this field also showed that areas with high acoustic impedance are correlated with low porosity values, whereas materials with high

porosities are observed in areas possessing low acoustic impedance. The trend plot of acoustic impedance shown in Fig. 19 indicates that under normal pressure conditions, acoustic impedance would increase linearly with depth, but certain intervals are abnormally pressured causing divergence of the supposed linear trend. This divergence

Fig. 17 Plot of pore pressure and interval transit time against depth for Well 3 showing concurrent increase of both parameters

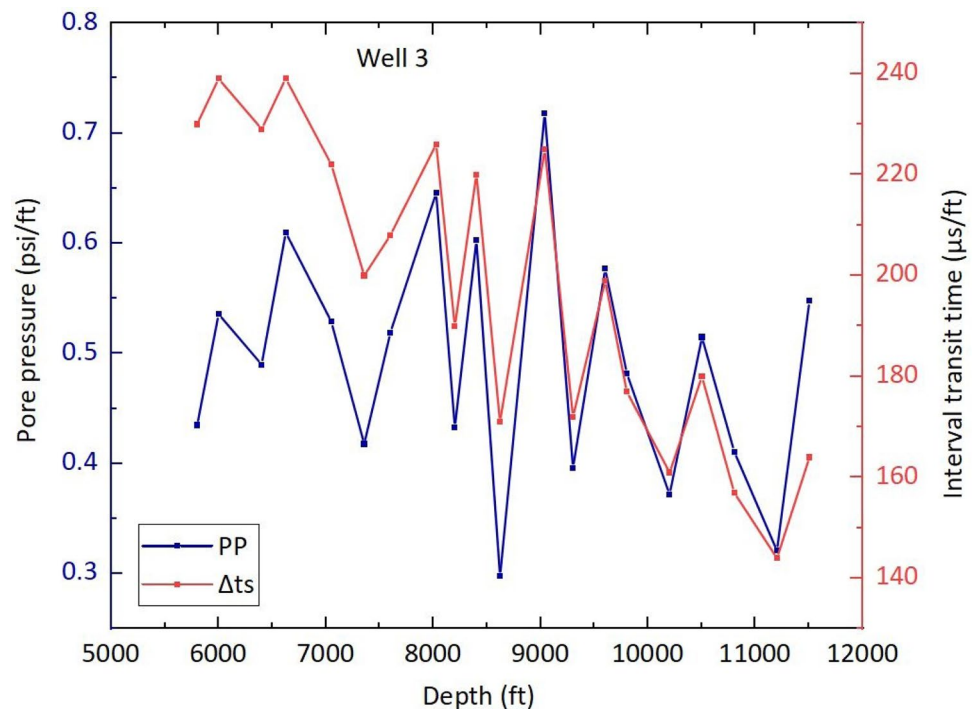
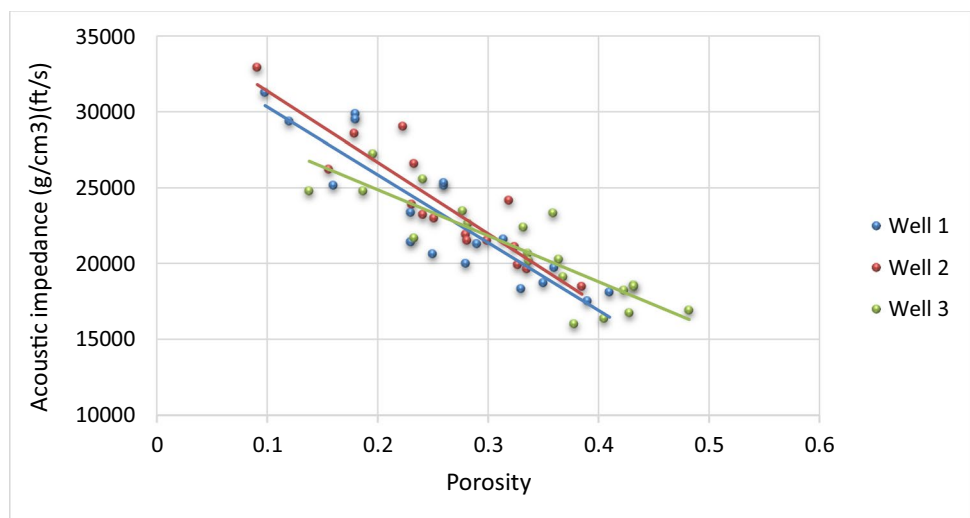


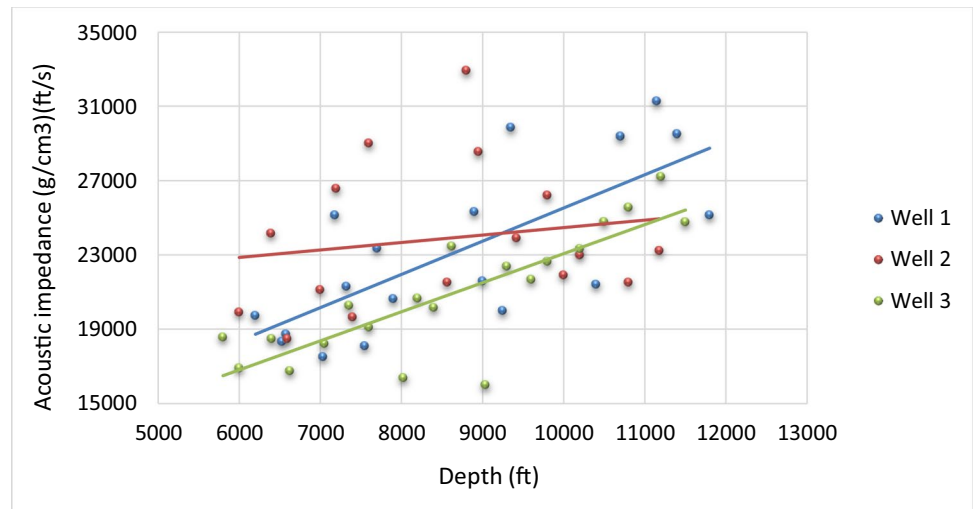
Fig. 18 Acoustic impedance against porosity for the three wells showing an imperfectly linear correlation



away from the linear trend increases with depth in the three wells, meanwhile, Well 3 appears to be more linearly correlated than the other two. Seemingly, inhomogeneity of the rock types may account for the scatter around the established best fit lines of regression since acoustic impedance values vary for shales and sands. Moreover, Avseth et al. (2001) reported that sands can be discriminated from shales by running acoustic impedance inversion, and such model can be applied to seismic data in predicting important anomalies which are related to hydrocarbons overpressure, tectonic history, sediments compaction and cementation.

The overall result in this study agrees with literature reports (e.g. Dutta 2002; Chopra and Huffman 2006; Cibin et al. 2008) indicating that overpressured intervals generally show the following properties: higher porosity, lower bulk density, lower effective stress, and lower velocities, both shear wave and compressional wave. Shales often exhibit large variations in petrophysical and mechanical properties, and the materials are intrinsically anisotropic because of large volume of clay minerals, hence, they are typically overpressured due to trapped fluids in pores, presence of organic materials, and low porosity and very low permeability (Dutta 2002; Peacock et al. 2011; Wang et al. 2012). In

Fig. 19 Depth trends of acoustic impedance for the three wells



this study, with an increasing shale content of the sediments, the effect lowers V_p and V_s but increases V_p/V_s . Overpressures in sedimentary basins are attributed to different mechanisms but the main causes are related to increasing formation stress and in-situ fluid generating mechanisms. It is believed that the tendency of these mechanisms and their processes to generate overpressure is dependent on the rock materials and fluid properties in the sedimentary rocks. Another important factor is the rate of change in properties and features under the normal basin conditions (Chopra and Huffman 2006). The dominant materials in Niger Delta Basin belong to Tertiary sediments. During the deposition of the materials, there was an increasing effect of vertical stress. Also, it is believed that the pore fluids escape while the pore spaces attempt compaction. Meanwhile, during sedimentation, grains of sediments are continuously building up on top of each other,

and as the thickness of the layer of sediment increases, the grains of the sediment are packed closer together, and at this time, some of the water is expelled from the pore spaces. Consequently, the most acceptable mechanism of overpressure generated in these processes is disequilibrium compaction. This phenomenon is responsible for the uneven distribution of rock physics and mechanical properties, thus, resulting in pore pressure rise and fall.

Generally, increase in pore pressure correspond to decrease in both shear and compressional velocities across the three wells. Seemingly, this effect is observed in the corresponding lowering of the impedance at these zones as the velocities and impedances of sands are much higher than for the overpressured layer which contains more of shale material (Avseth et al. 2001). The decrease in the P-wave velocity producing increased pore pressure has

Fig. 20 Composite Plot of Well 1 showing critical intervals with low elastic moduli and velocities yielding high pore pressure (arrows point at critical intervals)

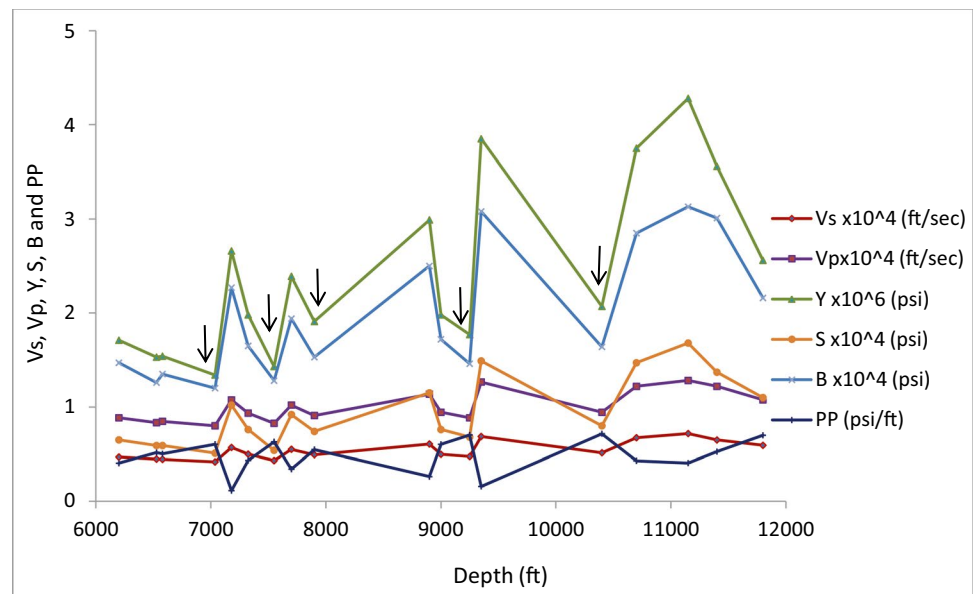


Fig. 21 Composite Plot of Well 2 showing critical intervals with low elastic moduli and velocities yielding high pore pressure (arrows point at critical intervals)

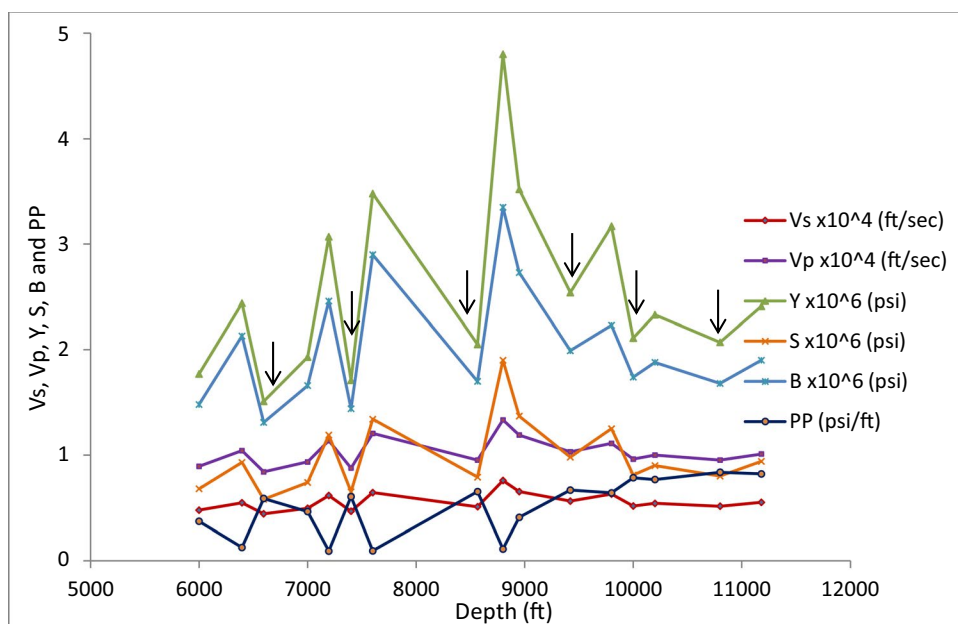
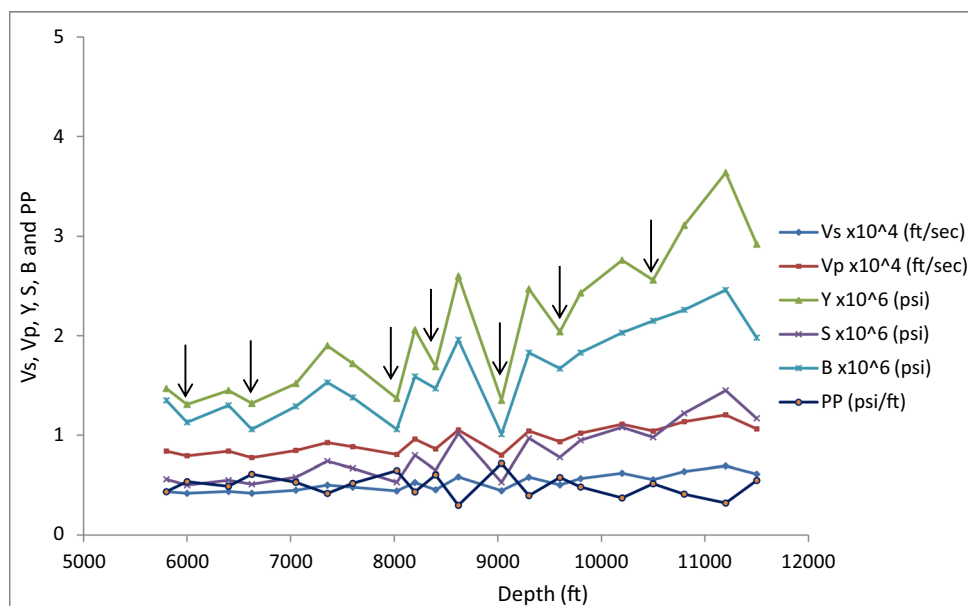


Fig. 22 Composite Plot of Well 3 showing critical intervals with low elastic moduli and velocities yielding high pore pressure (arrows point at critical intervals)



been used for detecting overpressure, consequently, the intervals showing abnormal trend in acoustic impedance plots are similarly assumed to have resulted from the abnormal pressure in the reservoir. Figures 20, 21 and 22 show composite plots of V_s , V_p , Y , B , S and PP against depth, where critical intervals corresponding to the zones with low velocities and high pore pressure encountered across the three wells have been identified using the black arrows. In Well 1, these intervals correspond to depth 7179 ft, 7700 ft, 7900 ft, 9350 ft, 10400 ft, and at greater depth. In Well 2, the abnormal pressure is found in depth 6595 ft, 7400 ft, 8566 ft, 9420 ft, and down depth. In Well 3,

the intervals are found in depth 6000 ft, 6625 ft, 8025 ft, 8400 ft and 9036 ft, 9600 ft.

The recurring subnormal pressure and overpressure noticed throughout in this field suggest non-uniform compaction of the Niger Delta formation. An inverse relationship which exists between pore pressure and elastic properties as well as velocities of waves is further established from results obtained. It is revealed that with increasing pore pressure, there is a corresponding decrease in the elastic properties of the rock and the velocities of waves. Hence, at every point where such decrease in V_s , V_p , Y , B , S commensurate with an increase in pore pressure, creating an abnormal pressure

zones, such intervals must be drilled carefully. Reports have shown that at such zones, there would be sanding problem when drilling, meanwhile, intervals with high geomechanical strength are strong enough to produce at high flow rates without sand. Therefore, sand control is highly essential for the intervals with low mechanical competency (Eyinla and Oladunjoye 2014), and it is highly essential to select adequate mud weight to ensure drilling safety, and to prevent hole collapses leading to fracture or losses.

Conclusions

This study has considered the behavioral patterns of material geomechanical properties in identifying overpressured intervals. It has been established that these overpressured intervals could be a serious threat to the successful implementation of enhanced recovery programs if not properly investigated. The values of estimated pore pressure from this study vary from well to well, but the general trend behaves the same across the three wells. Cross-plots of relevant rock properties such as density, velocity, mechanical properties, acoustic impedance, V_p/V_s and pore pressure produce patterns which confirm that the formation has been subjected to disequilibrium compaction. This is because of the uneven distribution of pressure across the three wells in which most of the intervals are abnormally pressured. It is concluded that pore pressure has a huge effect on the elastic moduli of the formations, as increase in pore pressure causes a decrease in the elastic properties. Elastic strength and velocities of the materials which ordinarily should follow an increasing order down depth varies at certain intervals because of the dominating abnormal pressure. In general, more stiff materials are at deeper depth, indicating that the less porous formations are stiffer than the porous layers.

The values of V_p/V_s were not only applicable for lithology identification, the correlation of both Poisson's ratio and the V_p/V_s has helped to ascertain the classification of lithology across the wells where high values indicate shale and overpressured intervals. Although the presence of gas can show the same signature as overpressure while interpreting V_p/V_s values, however, interval transit time has served as a useful tool in confirming the presence of overpressure as observed in this study. The velocity of shear and compressional wave is related to the material porosity, and the relationship has also helped in promoting overpressure detection. This study has reported that an obvious deviation from existing trends give a pointer to the type of reservoir material at such interval, and a possibility of overpressure have been inferred. From the overall geomechanical properties analyzed, it is safe to adduce that divergence of any supposed trend is an indication of abnormal pressure and optimum production can be achieved by targeting intervals with high

geomechanical strength, less shaly zones and normal pressure in the reservoir.

Nevertheless, the abnormal intervals can be carefully drilled safely and economically by adopting appropriate and suitable mud and casing. The drilling fluid's density must also be increased to preserve the wellbore pressure above the formation pore pressure in order to maintain hole stability, to prevent borehole collapse and to prevent the influx of formation fluids into the wellbore. This careful consideration can help to reduce downhole problems, loss of reserves, environmental pollution and loss of life which might be resulted from the abnormal pressure. However, the proper prediction and characterization of subsurface formations, the geomechanical characteristics and overpressure are important to know the landing interval for the lateral wells and how the fractures will propagate while maintaining stability during hydraulic fracturing. Also, if this method is carefully utilized, it can serve as an easy tool for predicting subsurface mechanical properties of formation, pressure study and understanding the relationships between each parameter, consequently, the problems associated with drilling petroleum wells in over-pressured sedimentary basins including blow out and wellbore instability can be prevented by taking the necessary precautions and using the required tools.

Conclusively, since this study has revealed various geomechanical and pressure properties as a result of changing state of sediments compaction, for any hydraulic fracturing program, a careful well planning and consideration of the pressured intervals is suggested, in order to improve the stimulation performance and well productivity. Correct designing of casing scheme can be employed to ensure optimum completion and maximum productivity. Meanwhile, although this study only considered vertical change in material properties of rocks, assuming homogeneities of the material laterally, it might be essential to investigate how lateral heterogeneities of rock would affect the material properties and possible pressure change, and their consequence during fluid injection or hydraulic fracturing program .

Funding Research funded by the African Union through Pan African University.

Compliance with ethical standards

Conflict of interest The authors declare that there is no conflict of interest regarding the publication of this paper.

Open Access This article is licensed under a Creative Commons Attribution 4.0 International License, which permits use, sharing, adaptation, distribution and reproduction in any medium or format, as long as you give appropriate credit to the original author(s) and the source, provide a link to the Creative Commons licence, and indicate if changes were made. The images or other third party material in this article are included in the article's Creative Commons licence, unless indicated

otherwise in a credit line to the material. If material is not included in the article's Creative Commons licence and your intended use is not permitted by statutory regulation or exceeds the permitted use, you will need to obtain permission directly from the copyright holder. To view a copy of this licence, visit <http://creativecommons.org/licenses/by/4.0/>.

References

- Abijah FA, Tse AC (2016) Geomechanical evaluation of an onshore oil field in the Niger Delta, Nigeria. *IOSR J Appl Geol Geophys* 4(1):99–111
- Al-Dousari M, Garrouch AA, Al-Omair O (2016) Investigating the dependence of shear wave velocity on petrophysical parameters. *J Pet Sci Eng* 146:286–296
- Archer S, Rasouli V (2012) A log-based analysis to estimate mechanical properties and in-situ stresses in a shale gas well in North Perth Basin. *WIT Trans Eng Sci*. <https://doi.org/10.2495/PMR120151>
- Assefa S, McCann C, Sothcott J (2003) Velocities of compressional and shear waves in limestones. *Geophys Prospect* 51(1):1–13. <https://doi.org/10.1046/j.1365-2478.2003.00349.x>
- Avseth P, Mavko, G, Dvorkin J, Mukerji T (2001) Rock physics and seismic properties of sands and shales as a function of burial depth. Presented at SEG Int'l Exposition and Annual Meeting San Antonio, Texas, 9–14 Sep 2001
- Avseth P, Flesche H, Wijngarden AV (2003) AVO classification of lithology and pore fluids constrained by rock physics depth trends. *Lead Edge* 22:1004–1011
- Azizi V, Memarian H (2015) Estimation of geomechanical parameters of reservoir rocks, using conventional porosity Log. Proc. 4th Asian Rock Mechanics Symposium, Rock Mechanics in Underground Construction. Retrieved from 17 Jul 2015
- Babu S, Sircar A (2011) A comparative study of predicted and actual pore pressures in Tripura India. *J Pet Technol Altern Fuels* 2(9):150–160
- Basu D, Ghosh DK, Paul A (1994) Determination of dynamic elastic properties of rocks and fracture pressure gradient from sonic waveforms. *Indian J Geol* 66(1):31–38
- Castagna JP, Batzle ML (1985) Eastwood RL Relationships between compressional-wave and shear-wave velocities in clastic silicate rocks. *Geophysics* 50:571–581
- Chen Z, Wang X, Atkinson A, Brandon N (2016) Spherical indentation of porous ceramics: cracking and toughness. *J Eur Ceram Soc* 36(14):3473–3480
- Chen Z, Ji Z, Huang H (2019) Acoustic impedance of perforated plates in the presence of bias flow. *J Sound Vib*. <https://doi.org/10.1016/j.jsv.2019.01.031>
- Chilingar GV, Serebryakov VA, Robertson JO (eds) (2002) Origin and prediction of abnormal formation pressures. Elsevier Publishing
- Chopra S, Huffman A (2006) Velocity determination for pore pressure prediction. *CSEG Rec* 31(4):28–46
- Chukwu GU (2017) Evaluation of geopressure regime in an onshore Niger delta field of Nigeria. *Biodivers Int J* 1(5):41–48
- Cibin P, Pizzaferrri L, Martera MD (2008) Seismic velocities for pore-pressure prediction. Some case histories. 7th international Conference and Exhibition on Petroleum Geophysics
- Cook J, Rene AF, Hasbo K, Green S, Judzis A, Martiu JW, Suarez-Rivera R, Jorg H, Hooyman P, Lee D, Noerth S, Sayers C, Koutsabelloulis N, Marsden R, Stage MG, Tan CP (2007) Rocks matter: ground truth in geomechanics. *Oil Rev* 2007:36–55
- Crain ERR (2013) Crain's petrophysical Handbook. Online shareware petrophysics training and reference manual. <https://www.spec2000.net/01-introduction.htm>
- Denney D (2011) 3D Geomechanical modeling of optimizes drilling in the Llanos Orientales basin, Columbia. *J Pet Technol* 63(9):86–88
- Dolberg DM, Helgesen J, Hanssen TH, Magnus I, Saigal G, Pedersen BK (2000) Porosity prediction from seismic inversion, Lavrans Field, Halten Terrace, Norway. *Lead Edge* 19(4):392–399
- Donaldson EC, Alam W, Begum N (2013) Rock Mechanics of Fracturing. In: *Hydraulic Fracturing Explained*. Elsevier, pp. 47–76. <https://doi.org/10.1016/b978-1-933762-40-1.50012-x>
- Atlas Dresser (1982) Well logging and interpretation techniques. The course for home study. Dresser Atlas Publication, Houston
- Dutta NC (2002) Geopressure prediction using seismic data: Current status and road ahead. *Geophysics* 67:2012–2041
- Emudianughe JE, Ogarue DO (2018) Investigating the subsurface pressure regime of ada-field in onshore Niger Delta Basin Nigeria. *J Geol Geophys*. <https://doi.org/10.4172/2381-8719.1000452>
- Eshkalak MO, Mohaghegh SD, Esmaili S (2014) Geomechanical properties of unconventional shale reservoir. *J Pet Eng* 2014:1–10. <https://doi.org/10.1155/2014/961641>
- Eyinla DS, Oladunjoye MA (2014) Estimating geo-mechanical strength of reservoir rocks from well logs. *J Environ Earth Sci* 4(20):38–43
- Eyinla DS, Oladunjoye MA (2018) Empirical analysis for the characterization of geo-mechanical strength and pressure regime: implications on hydraulic fracturing stimulation. *Petroleum*. <https://doi.org/10.1016/j.petlm.2018.05.002>
- Fan Z, Eichhubl P, Gale JFW (2016) Geomechanical analysis of fluid injection and seismic fault slip for the Mw4.8 Timpson, Texas, earthquake sequence. *J Geophys Res Solid Earth* 121(4):2798–2812. <https://doi.org/10.1002/2016JB012821>
- Feng J, Li L, Jin J, Dai J, Luo P (2018) An improved geomechanical model for the prediction of fracture generation and distribution in brittle reservoirs. *PLoS One* 13(11):e0205958. <https://doi.org/10.1371/journal.pone.0205958>
- Garia S, Pal AK, Ravi K, Nair AM (2019) A comprehensive analysis on the relationships between elastic wave velocities and petrophysical properties of sedimentary rocks based on laboratory measurements. *J Pet Explor Prod Technol*. <https://doi.org/10.1007/s1320-019-0675-0>
- Gidley JL, Holditch SA, Nierode DE, Jnr Veatch RW. (1989) Recent advances in hydraulic fracturing. *SPE Monogr* 12:1–38
- Gudmundsson A (2004) Effects of Young's modulus on fault displacement. *C R Geosci* 336(1):85–92. <https://doi.org/10.1016/j.crte.2003.09.018>
- Guo B, Lyons WC, Ghalambor A (2007) Hydraulic fracturing. *Pet Prod Eng*. <https://doi.org/10.1016/b978-075068270-1/50023-2>
- Ismail AR (2010) Ch 5 Formation pressures - SKPP 3413 Drilling Engineering. In: *Petroleum Engineering Dept. Faculty of Petroleum & Renewable Energy Eng, University Teknologi Malaysia*. <https://www.coursehero.com/file/23900809/Ch-5-Formation-pressures/>
- Ispas I, Eve R, Hickman RJ, Keck RG, Willson SM, Olson KE (2012) Laboratory testing and numerical modelling of fracture propagation from deviated wells in poorly consolidated formations. *Soc Pet Eng*. <https://doi.org/10.2118/159262-MS>
- Josh M, Esteban L, Piane CD, Sarout J, Dewhurst DN, Clennell MB (2012) Laboratory characterisation of shale properties. *J Pet Sci Eng* 88–89(2):107–124
- Kahraman S, Yeken T (2008) Determination of physical properties of carbonate rocks from P-wave velocity. *Bull Eng Geol Environ* 67:277–281
- Kolawole O, Federer-Kovács G, Szabó I (2018) Formation susceptibility to wellbore instability and sand production in the Pannonian Basin, Hungary. In: *American Rock Mechanics Association, Presented at the 52nd US Rock Mechanics/Geomechanics Symposium held in Seattle, Washington, USA*

- Kolawole O, Ispas I (2019) Interaction between hydraulic fractures and natural fractures: current status and prospective directions. *J Pet Explor Prod Technol*. <https://doi.org/10.1007/s13202-019-00778-3>
- Kukla PA, Reuning L, Becker S, Urai JL, Schoenherr J (2011) Distribution and mechanisms of overpressure generation and deflation in the late Neoproterozoic to early Cambrian South Oman Salt Basin. *Geofluids* 11(4):349–361. <https://doi.org/10.1111/j.1468-8123.2011.00340.x>
- Kumar D, Hoversten GM (2012) Geophysical model response in a shale gas. *Geohorizons* 17:31–37
- Kumar M, Dasgupta R, Singha DK, Singh NP (2017) Petrophysical evaluation of well log data and rock physics modeling for characterization of Eocene reservoir in Chandmari oil field of Assam-Arakan basin India. *J Petrol Explor Prod Technol*. <https://doi.org/10.1007/s13202-017-0373-8>
- Ichenwo JL, Olatunji A (2018) pore pressure and fracture pressure forecast in Niger Delta. *Int J Eng Res Technol (IJERT)* 7(04):338–344
- Lal M (1999) Shale stability: drilling fluid interaction and shale strength, SPE Latin American and Caribbean Conference.
- Law BE, Spencer CW (1998) Abnormal pressure in hydrocarbon environments. In: Law BE, Ulmishek GF, Slavin VI (eds) *Abnormal pressure in hydrocarbon environments*. American Association of petroleum Geologists Memoir, Oklahoma, pp 1–11
- Li Q, Chen M, Jin Y, Zhou Y (2013) Rock mechanical properties of shale gas reservoir and their influences on hydraulic fracture. Presented at the International Petroleum Technology Conference held in Beijing, China, 26–28 Mar 2013. IPTC 16580 pp 1-9.
- Li J, Lu S, Xue H, Xie L, Zhang P (2015) Quantitative evaluation on the elastic property of oil-bearing mudstone/shale from a Chinese continental basin. *Energy Explor Exploit* 33(6):851–868
- Liu Y, Zhuoheng C, KezhenH (2012) Shear velocity prediction and its rock mechanic implications. Paper presented at CSPG/CSEG/CWLS GeoConvention 2012, (Vision) Calgary TELUS convention centre & ERCB Core Research Centre, Calgary, AB, Canada
- Maleki S, Moradzadeh A, Riabi RG, Gholami R, Sadeghzadeh F (2014) Prediction of shear wave velocity using empirical correlations and artificial intelligence methods. *NRIAG J Astron Geophys* 3(1):70–81. <https://doi.org/10.1016/j.nrjag.2014.05.001>
- Maulianda B, Prakasan A, Wong RC-K, Eaton D, Gates ID (2019) Integrated approach for fracture characterization of hydraulically stimulated volume in tight gas reservoir. *J Pet Explor Prod Technol*. <https://doi.org/10.1007/s13202-019-0663-4>
- McKee CR, Bumb AC, Bell GJ (1984) Effects of stress-dependent permeability on methane production from deep coalseams. Paper SPE 12858, presented at the Unconventional Gas Recovery Symposium, Pittsburgh, Pennsylvania, May 1984.
- Miller SLM, Stewart RR (1990) Effects of lithology, porosity and shaliness on P- and S-wave velocities from sonic logs. *Can J Explor Geophys* 26:94–103
- Nwozor KK, Omudu ML, Ozumba BM, Egbuachor CJ, Onwuemesi AG, Anike OL (2013) Quantitative evidence of secondary mechanisms of overpressure generation: insights from parts of onshore Niger Delta Nigeria. *Pet Technol Dev J* 3(1):64–83
- Nwozor KK, Onuorah LO, Onyekuru SO, Egbuachor CJ (2017) Calibration of gardner coefficient for density–velocity relationships of tertiary sediments in Niger Delta Basin. *J Pet Explor Prod Technol* 7(3):627–635. <https://doi.org/10.1007/s13202-017-0313-7>
- Ogunsakin OM, Ehinola AO, Olopade E (2019) Pressure regime, pressure regression detection and implications in the SMK field, Onshore, Western Niger Delta Nigeria. *Asian J Earth Sci* 12(1):1–12. <https://doi.org/10.3923/ajes.2019.1.12>
- Osinowo OO, Oladunjoye MA, Olayinka AI (2015) Overpressure prediction from seismic data and the implications on drilling safety in the Niger Delta, Southern Nigeria. *Pet Technol Dev J* 5(2):13–26
- Owolabi OO, Okpobiri GA, Obomanu IA (1990) Prediction of abnormal pressures in the niger delta basin using well logs. Paper presented at SPE Conference 10–13 Jun 1990, paper No. CIM/SPE 90-75.
- Peacock SM, Christensen NI, Bostock MG, Audet P (2011) High pore pressures and porosity at 35 km depth in the Cascadia subduction zone. *Geology* 39(5):471–474. <https://doi.org/10.1130/g31649.1>
- Pickett GR (1963) Acoustic character logs and their applications in formation evaluation. *J Pet Technol* 15(6):659–667
- Saputro NE, Haris A (2017) 3D Geomechanical modeling driven by acoustic impedance and seismic velocity: a case study of carbonate reservoir, East Java Basin. Proceedings of the 3rd International Symposium on Current Progress in Mathematics and Sciences 2017 (ISCPMS2017) AIP Conference Proceeding 2023, 020253-1–020253-4; <https://doi.org/10.1063/1.5064250>
- Saikia K, Ikuku CE, Sarkar BC (2018) An integrated approach to discretized 3D modeling of geomechanical properties for unconventional mature field appraisal in the western Canadian sedimentary basin. *J Pet Explor Prod Technol* 8:417–429. <https://doi.org/10.1007/s1320-017-0406-3>
- Satti IA, Ghosh D, Yusoff WIW, Hoesni MJ (2015) Origin of overpressure in a field in the southwestern malay basin. *SPE Drill Complet* 30(3):198–211
- Shafiq MU, Mahmud HB (2017) Sandstone matrix acidizing knowledge and future development. *J Pet Explor Prod Technol* 7(4):1205–1216. <https://doi.org/10.1007/s13202-017-0314-6>
- Saikia K, Ikuku CE, Sarkar BC (2018) An integrated approach to discretized 3D modeling of geomechanical properties for unconventional mature field appraisal in the western Canadian sedimentary basin. *J Pet Explor Prod Technol* 8:417–429. <https://doi.org/10.1007/s13202-017-0406-3>
- Satter A, Iqbal GM (2016) Reservoir engineering—the fundamentals, simulation, and management of conventional and unconventional recoveries. In: Gulf Professional Publishing, pp 29-79. <https://doi.org/10.1016/B978-0-12-800219-3.00003-6>
- Shafiq MU, Mahmud HKB, Zahoor MK, Shahid ASA, Rezaee R, Arif M (2019) Investigation of change in different properties of sandstone and dolomite samples during matrix acidizing using chelating agents. *J Pet Explor Prod Technol*. <https://doi.org/10.1007/s13202-019-0683-0>
- Stacher P (1995) Present understanding of the niger delta hydrocarbon habitat. In: Oti MN, Postma G (eds) *Geology of deltas*. Balkema, Rotterdam
- Streit JE, Hillis RR (2004) Estimating fault stability and sustainable fluid pressures for underground storage of CO₂ in porous rock. *Energy* 29(9–10):1445–1456. <https://doi.org/10.1016/j.energy.2004.03.078>
- Swarbrick RE, Osborne MJ (1998) Mechanisms that generate abnormal pressure an overview. In: Law BE, Ulmishek GF, Slavin VS (eds) *Abnormal pressures in hydrocarbon environments*. AAPG Memoir, Oklahoma
- Taheri-Shakib J, Ghaderi A, Nik MAS (2019) Numerical study of influence of hydraulic fracturing on fluid flow in natural fractures. *Petroleum* 5(2019):321–328. <https://doi.org/10.1016/j.petlm.2018.10.005>
- Tatham RH (1982) Vp/Vs and Lithology. *Geophys* 47:336–344. <https://doi.org/10.1190/1.1441339>
- Telford WM, Geldart LP, Sheriff RE (1990) *Applied geophysics*. Cambridge University Press, Cambridge, p 645
- Tenthorey E, Cox SF, Todd HF (2003) Evolution of strength recovery and permeability during fluid–rock reaction in experimental fault zones. *Earth Planet Sci Lett* 206(1–2):161–172. [https://doi.org/10.1016/s0012-821x\(02\)01082-8](https://doi.org/10.1016/s0012-821x(02)01082-8)
- Turner JP, Healy D, Hillis RR, Welch MJ (2017) Geomechanics and geology. *Geol Soc Lond Spec Publ* 458:7–29. <https://doi.org/10.1144/SP458.7>
- Tuttle MLW, Charpentier RR, Brownfield ME (1999). The niger delta petroleum system: niger delta province, nigeria cameroon, and equatorial guinea, Africa. Open-File Report 99-50-H, 1999

- Udo KI, Akpan MJ, Agbasi OE (2015) Estimation of overpressures in onshore niger delta using wire-line data. *Int J Sci Res* 4(5):2780–2784
- Uyanik O (2010) Compressional and shear-wave velocity measurements in unconsolidated top soil and comparison of the results. *Int J Phys Sci* 5(7):1034–1039
- Vilarrasa V, Makhnenko R, Gheibi S (2016) Geomechanical analysis of the influence of CO₂ injection location on fault stability. *J Rock Mech Geotech Eng* 8(2016):805–818. <https://doi.org/10.1016/j.jrmge.2016.06.006>
- Wang Q, Ji S, Sun S, Marcotte D (2009) Correlations between compressional and shear wave velocities and corresponding Poisson's ratios for some common rocks and sulfide ores. *Tectonophysics* 469(1–4):61–72. <https://doi.org/10.1016/j.tecto.2009.01.025>
- Wang X-Q, Schubnel A, Fortin J, David EC, Guéguen Y, Ge H-K (2012) High V_p/V_s ratio: saturated cracks or anisotropy effects? *Geophys Res Lett*. <https://doi.org/10.1029/2012gl051742>
- Wang R, Ding W, Zhang Y, Wang Z, Wang X, He J, Zeng W, Dai P (2016) Analysis of developmental characteristics and dominant factors of fractures in Lower Cambrian marine shale reservoirs: a case study of Niutitang formation in Cen'gong block, southern China. *J Pet Sci Eng* 138:31–49. <https://doi.org/10.1016/j.petrol.2015.12.004>
- Xue Y, Cheng L, Mou J, Zhao W (2014) A new fracture prediction method by combining genetic algorithm with neural network in low-permeability reservoirs. *J Pet Sci Eng* 121:159–166. <https://doi.org/10.1016/j.petrol.2014.06.033>
- Zhang J, Lang J, Standifird W (2009) Stress, porosity, and failure-dependent compressional and shear velocity ratio and its application to wellbore stability. *J Pet Sci Eng* 69(3–4):193–202. <https://doi.org/10.1016/j.petrol.2009.08.012>
- Zhang JJ (2019) Pore pressure prediction and monitoring. *Appl Pet Geomech*. <https://doi.org/10.1016/b978-0-12-814814-3.00008-3>
- Zhou J, Huang H, Deo M (2016) Simulation of hydraulic and natural fracture interaction using a coupled DFN-DEM model. American Rock Mechanics Association, Houston, Texas

Publisher's Note Springer Nature remains neutral with regard to jurisdictional claims in published maps and institutional affiliations.